Published in final edited form as:
Nanoscale. 2012 July 21; 4(14): 4269–4274. doi:10.1039/c2nr30773a.

$Ag_{44}(SR)_{30}^{4-}$:a silver-thiolate superatom complex

Kellen M. Harkness[1,‡], **Yun Tang**[2,‡], **Amala Dass**[3], **Jun Pan**[4], **Nuwan Kothalawala**[3], **Vijay J. Reddy**[3], **David E. Cliffel**[1], **Borries Demeler**[5], **Francesco Stellacci**[2], **Osman M. Bakr**[4,*], and **John A. McLean**[1,*]

[1]Department of Chemistry, Vanderbilt Institute of Chemical Biology, Vanderbilt Institute for Integrative Biosystems Research and Education, Vanderbilt University, 7330 Stevenson Center, Station B 351822, Nashville, TN USA 37235, tel : +1.615.322.1195 [2]Institute of Materials, EcolePolytechniqueFederale de Lausanne, Switzerland [3]Department of Chemistry and Biochemistry, University of Mississippi, University, Mississippi 38677, United States [4]Division of Physical Sciences and Engineering, Solar and Photo-voltaics Engineering Center, King Abdullah University of Science and Technology (KAUST), Thuwal 23955-6900, Saudi Arabia [5]Department of Biochemistry, The University of Texas Health Science Center at San Antonio, San Antonio, TX 78229, USA

Abstract

Intensely- and broadly-absorbing nanoparticles (IBANs)of silver protected by arylthiolates were recently synthesized and showed unique optical properties, yet question of their dispersity and their molecular formulas remained. Here IBANs are identified as a superatom complex with a molecular formula of $Ag_{44}(SR)_{30}^{4-}$ and an electron count of 18.This molecular character is shared by IBANs protected by 4-fluorothiophenol or 2-naphthalenethiol. The molecular formula and purity is determined by mass spectrometry and confirmed by sedimentation velocity-analytical ultracentrifugation. The data also give preliminary indications of a unique structure and environment for $Ag_{44}(SR)_{30}^{4-}$.

Introduction

Ultrasmall, atomically monodisperse, thiolate-protected metal nanoparticles(NPs) constitute a new class of compoundsthat has gained attention because of their unique and entirely novel optical,[1-3] electronic,[4-6] and structural properties.[7-10] This class occupies the chemical space that bridges small inorganic molecules and larger (>2 nm core diameter) monolayer-protected metal nanoparticles, with properties that are reflective of both bulk and molecular materials. The smallest possess less than 10 metal atoms[11,12] and are easily distinguished by their strong scattering of UV electromagnetic radiation through quantum effects.[2] The largest have very recently been discovered to exhibit evidence of a surface plasmon,[13,14] a classic property of the bulk metal.

The most fundamental unifying property of these nanomaterials is their stability relative to nanoparticles of similar molecular formula. Depending on the conditions of cluster formation, the metal atoms will find potential energy minima which correspond to so-called

*john.a.mclean@vanderbilt.edu, osman.bakr@kaust.edu.sa.
‡These authors contributed equally to the paper.

Electronic Supplementary Information (ESI) available:. Extended mass spectra and SV-AUC data. See DOI:10.1039/b000000x

"magic sizes." Reductive syntheses of metalnanoparticles in the presence of thiols under ambient conditions can yield thiolate-protected, magic-sized nanoclusters.

Understanding the nature of magic sizes for these thiolate-protected metal NPs has been the object of intense research.[15,16] The synthesis of monodispersemagic-sized nanoparticles has facilitated their crystallization and structural determination, which allowed for the first time a theoretical understanding of the origins of their optical and magnetic behaviour. An excellent case study is $Au_{25}(SCH_2CH_2Ph)_{18}$.

Though its approximate size was known for some time,[1,17] it was not until 2007 that its true molecular identity was elucidated by mass spectrometry (MS).[18-21]_ENREF_18 Density functional theory (DFT) calculations predicted[22] and X-ray crystallography confirmed[8] a minimized-energy structure soon thereafter. For Au_{25}(glutathione)$_{18}$, early mass spectrometric experiments[23] culminated in the precise measurement of molecular identity,[24] followed by study of its structure and properties.[25,26] A similar story is also emerging for thiolate-protected silver nanoclusters: early reports of monodisperse AgNPs[27-29] have led to precise characterization.[11,12,30-32]

Hakkinen and co-workers laterdefined a subclass of magic-sized gold nanoclusters as superatom complexes (SCs).[33,34] This nomenclature reflects the fact that the materials are not elemental in nature, but rather complexes of a metal cluster with electron-localizing organic ligands. SCs are defined by theiratom-like properties, with unique optical and electronic properties caused by the emergence of discrete molecular orbitals with gaps in the near-IR to near-UV range. SCs are distinguished from magic-sized NPs that do not have an electronically closed shell.[11,12,35] Shell closing occurs at certain known electron count numbers, *i.e.,* 2, 8, 18, 34, 58, *etc.* Electron counts are calculated by the following equation:[33]

$$n^* = N\nu_A - M - z \quad (1)$$

where n^* is theelectron count for the superatom complex, N is the number of metal atoms, ν_A is the valence of the metal atoms ($1e^-$ for Ag or Au), M is the number of ligands, and z is the overall charge.

Some of usrecently reported the synthesis of arylthiol-protected Ag nanoclusters, referred to as intensely- and broadly-absorbing nanoparticles (IBANs), that possesseight well-resolved non-plasmonic optical transitions in linear absorption spectra, with a HOMO-LUMO gap of ~1.5 eV.[36] Synthesized through multiple temperature-controlled reduction steps, IBANsare stable in solution at −4°C for several months. The IBANs were estimated to have an average core diameter of ~1.3 nm based on wide-angle X-ray diffraction and preparative ultracentrifugation data. Upon heating, the nanoclusters grow into larger nanoparticles (~2nm) with a single plasmon-like absorption band. Theoptical spectra contain a number of unique absorbance bands, reflecting electronic transitions that are indicative of an SC. However, given the complexity of the spectra, the monodispersity and true molecular identity of the IBANs remained in question.

In this report, we present evidence that IBANs are a monodisperse SC, with an observable closed electronic shelland a single dominant molecular formula. Data which support this conclusion were obtained by sedimentation velocity-analytical ultracentrifugation (SV-AUC) and electrospray ionisation-mass spectrometry (ESI-MS). These platforms were chosen for their ability to allow investigation of IBAN size and monodispersity of without disturbing their native structure.

Methods

2-NPT- and 4-FTP-stabilized IBANs were synthesized in dimethylformamide (DMF) according to the procedures described previously[36] and purified by Sephadex® LH-20. All mass spectra were collected by using Waters Synapt G2 equipped with an electrospray ionization (ESI) source. The IBAN samples in DMF were diluted 1:8(v/v) ratio with acetonitrile (HPLC grade). Sodium iodide was used as an external mass calibrant. The instrument was operated in negative sensitivity mode. Capillary voltage was set to −2.3 kV, extraction cone voltage to 7.4, and sampling cone voltage was set at 10. Higher settings for the sampling cone voltage were found to increase the abundance of fragment ions (Figure S1). Source and desolvation temperatures were 100 and 150 °C, respectively. All mass spectral data were processed using MassLynx v4.1 software (Waters Corp., Milford, MA, USA). Experiments were reproducible on a Waters Synapt G1 HDMS in dual reflectron mode with higher sampling cone voltage settings (≥40). Calculated spectra were obtained using Data Explorer v4.3 software (Applied Biosystems, Foster City, CA, USA).

SV-AUC experiments were carried out on an Optima XL-A analytical ultracentrifuge from Beckman Coulter with an absorbance optical detection system and An-60 Ti rotor. Sample solutions (440 μL) were loaded in double-sector centre pieces with quartz windows. One sector contained an IBAN solution in DMF with a concentration adjusted so that the absorbance at the monitored wavelength (423 nm) was in the linear range for Beer's law (0.5 to 1 OD). A reference pure DMF solvent was loaded in the sector adjacent to the sample solution. Aluminium centre pieces were used due to chemical compatibility considerations with DMF. IBAN solutions were centrifuged at rotor speeds of 60,000 rpm at a temperature of 20 °C. The samples and rotor were left in the centrifuge for about 5 to 6 hours in order for the temperature to equilibrate before the experiments were initiated. Sedimentation profiles were acquired by scanning the sectors in 0.003 cm radial increments. The average time required to scan an entire sector was about 1 minute. Approximately 189 sedimentation profiles were analysed for time-invariant and radial-invariant noise subtraction, and Lamm equation modelling using Ultrascan III_ENREF_2 (revision 1244, see Figure S2).[37] The noise subtraction was performed by 2-dimensional spectrum analysis (2DSA)[38] with meniscus optimization.[39] Sedimentation-diffusion distributions were obtained after genetic algorithm[40,41] optimization and Monte Carlo analysis,[42] assuming non-interacting particles.

Results and discussion

Taking advantage of the versatility of the multiple temperature-controlled reduction method,[36] two sets of IBANs protected by 2-NPT and 4-FTP respectively were chosen as model systems for characterization. Synthetic products were consistent with previous IBANs (Figure 1).[36] In the absence of crystallographic data, the best method for characterizing the IBANs with atomic precision is ESI-MS. With the mass accuracy and resolution afforded by modern instrumentation, the charge of an IBAN and the precise number of metal atoms and thiolate ligands can be determined unequivocally. Because of these capabilities, MS has been a vitally important technique for the study of magic-sized, thiolate-protected metal NPs.[11,18,20,26,30,43-53]

For both IBAN samples, the same metal-thiolate stoichiometry was observed by ESI-MS: $Ag_{44}(SR)_{30}^{4-}$ (Figure 1). Even in the low-energy ESI process, the use of insufficiently lowcapillary and cone voltage settings produces in-source fragmentation (Figure S1). Product ions predominantly undergo a loss of $Ag(SR)_2^-$ to form $Ag_{43}(SR)_{28}^{3-}$. The electron number calculated for the intact $Ag_{44}(SR)_{30}^{4-}$ and the dominant fragment $Ag_{43}(SR)_{28}^{3-}$ is 18 (Equation 1), corresponding to a closed electron shell. Notably, low-abundance ions were observed with different molecular formulae (Figure S1). These ions correspond to

$Ag_{44}(SR)_{30}^{4-}$ or $Ag_{43}(SR)_{28}^{3-}$ with one or two additional silver atoms or thiolate ligands. Any ion with an electron number other than 18 is ≤5% abundance relative to $Ag_{44}(SR)_{30}^{4-}$.

SV-AUC, an orthogonal characterization technique, provides confirmation of monodispersity and approximate size. In this technique, particles in solution are subjected to large gravitational force fields in the centrifuge, leading to sedimentation. The velocity of sedimentation is determined by the molecular weight, shape, surface properties, and density of the particle. Because detection is performed using optical absorption measurements, this technique is non-destructive. After measurements are made, a simple hydrodynamic model is applied to convert sedimentation velocity to sedimentation and diffusion coefficients. The number of Ag atoms (N_{Ag}) and thiol molecules (N_{SR}) in the cluster can be inferred from theexperimentally measured density (ρ_p) and molecular weight (MW_p) according to the relationships:[54]

$$N_{Ag} = \frac{\left(\frac{MW_p}{\rho_p}\right) - \left(\frac{MW_p}{\rho_{SR}}\right)}{AW_{Ag}\left(\frac{1}{\rho_{Ag}} - \frac{1}{\rho_{SR}}\right)} \quad (2)$$

where AW_{Ag} is the atomic weight of Ag, 107.86 g/mol,MW_{SR} is the deprotonated molecular weight of the thiolate,ρ_{Ag} is the density of the silver core, and ρ_{SR} is the density of the ligand, (*e.g.*, $\rho_{2\text{-}NPT}$=1.1 g/cm^3),[55] respectively. This gentle technique has been demonstrated to provide an unparalleled amount of information for gold-thiolate SCs and larger nanoparticles in a single platform.[54]

After noise subtraction and modelling (Figure S2), sedimentation coefficient (S) and diffusivity (D) distributionswere generated for 2-NPT IBANs in DMF (Figure 2). Approximately 94% of the sample is comprised of one specie with S= 3.68×10^{-13} s and D=1.714×10^{-6} cm^{2}s^{-1}. In addition, a small fraction (~6%) of the species sediments at a much faster rate (S~12.4×10^{-13} s). Closer analysis of the sedimentation boundary suggests that the particles are slightly interacting, which implies that the faster-sedimenting species are aggregates of the primary particles. Further evidence in support of this argument can be found in the extrapolation plot for the enhanced van Holde-Weischet (vHW) analysis (Figure 3).[56] The data show an apparently homogeneous sample with slight concentration-dependent non-ideal solution behaviour. This is indicated by the crossing over of the extrapolation lines (near the '*' symbol), which suggests that particles sedimenting in the higher concentration region of the boundary sediment slower than particles sedimenting at lower concentration in the lower part of the sedimentation boundary.[57] The above analysis of the SV-AUC experiment is strong evidence that the IBANs are an atomically monodisperse cluster.

Based on the measured S and D values we estimate that 2-NPT-IBANs have a molecular weight *ca.* 11.2 kDa, with a density of 1.78 g/cm^3,N_{Ag}≈44 atoms, and $N_{2\text{-}NPT}$≈40 ligands; suggesting that the IBANs have an approximate formula *ca.*$Ag_{44}(SR)_{40}$. Unfortunately, the relative error in the estimated MW was ~18% due to the significant particle-particle interaction observed during sedimentation, which was not the case for thiolated gold clusters characterized in previous work (Table S1).[54] Nevertheless, SV-AUC confirmed the identity of the IBANs as a monodisperse but labile ~10 kDa nanomaterial, strongly supporting the interpretation of the more accurate mass spectra.

On the properties of $Ag_{44}(SR)_{30}^{4-}$

Armed with the data presented here and the body of evidence that has been accumulated on metal-thiolate SCs, some comments can be made concerning the structural and electronic

properties of $Ag_{44}(SR)_{30}^{4-}$. Many of the most stable thiolate-protected gold nanoclusters (*e.g.*, $Au_{25}(SCH_2CH_2Ph)_{18}^{-}$) combine electronic and geometric sources of stability, with a closed electron shell and highly symmetric structure. However, recent evidence has suggested that geometric factors are dominant in determining stability for some gold-thiolate SCs.[58] _ENREF_47 Thus the geometric structure of $Ag_{44>}(SR)_{30}^{4-}$ may be the primary source of its stability.

The number of thiolate ligands protecting an SC of this size is remarkable. Based on the recently described scaling law for nanoclusters,[59]

$$N_{SR}=\frac{\left(\frac{MW_p}{\rho_{Ag}}\right)-\left(\frac{MW_p}{\rho_p}\right)}{MW_{SR}\left(\frac{1}{\rho_{Ag}}-\frac{1}{\rho_{SR}}\right)} \quad (3)$$

the number of ligands (L) scales with the number of metal atoms (N). The y-intercept (m) serves as a convenient term for the comparison of NP shapes and ligand coverage. It was found that for thiolate-protected gold nanoclusters with a known molecular formula, the average $m = 2.08$. For $Ag_{44}(SR)_{30}^{4-}$, $m = 2.41$, a higher value than for any known gold-thiolate nanoclusters. As the shape of the cluster is one determining factor of m,[59] the high value could be indicative of structure with a relatively high aspect ratio. Such anisotropyyields increased surface area and additional binding sites for metal-thiolate protecting groups, similar to that observed for theprolate $Au_{38}(SCH_2CH_2Ph)_{24}$ (m = 2.12).[60,61] However, a high aspect ratiois not supported by other data.[36]

The relatively thiolate-rich character could also reflect differences between silver- and gold-thiolate interfaces. The organization of self-assembled monolayers on two-dimensional silver and gold surfaces are known to be different,[62] but the true structure of silver-thiolate interfaces on nanoparticles has not been experimentally determined. The fragmentation of $Ag_{44}(SR)_{30}^{4-}$ to yield predominantly $Ag_{43}(SR)_{28}^{3-}$ (loss of $Ag(SR)_2^{-}$ complex, Figure S1) rather than $Ag_{44}(SR)_{29}^{3-}$ (loss of SR^{-}) could be considered evidence of the presence of silver-thiolate protecting complexes analogous to those found on gold-thiolate SCs.[53,63] The large number of thiolates present may indicate a favoured structure in which Ag-thiolate protecting groups possess a ~1:1 metal:thiolate stoichiometric ratio, rather than the 1:2 to 2 : 3 range observed for gold-thiolate SCs.[7,8,60] _ENREF_57 _ENREF_7 The electronegativity of silver is also significantly less than that of gold (χ = 1.93 and 2.54, respectively),[64] while arylthiolligandsare more electronegative than commonly-used phenylethanethiol.[46,65] The large number of thiolates should enhance stability for the SC by providing additional electron localization and steric protection. _ENREF_7

The charge state of $Ag_{44}(SR)_{30}^{4-}$ is extraordinary among metal-thiolate SCs. Observed charge states in excess of ±2 are normally only achievedby electrochemical methods[5,66] or by the use of ligands that bear charge.[18,19,25,67] The fixed charge of the IBANs has a strong effect on interactions between the nanoclusters and their environment, increasing solubility in polar aprotic solvents such as DMF[68] and attracting counterions to the IBAN surface. The associating counterions appear to be principally Ag^{+}, as evidenced by the presence of Ag-IBAN adducts in the mass spectra (Figure S1). No cationssuch as tetraoctylammonium (TOA^{+}) were used during synthesis, and no electrolytes were added for MS analysis. Sodium may also be present, but Na-IBAN adducts were not observed in mass spectra.

The IBAN environment is suitable for cation-π interactions. The anionic nature of the IBAN and the electron-donating behaviour of the silver core will further strengthen these interactions.[69,70] The significant surface curvature of IBANs will lead to more exposed

aromatic groups in the organic layer, yielding opportunities for favourable interaction geometries between multiple ligands and free metal ions.[71,72]

Silver nanoparticles are known to be less noble than their gold analogues,[73] and the lability of $Ag_{44}(SR)_{30}^{4-}$ is apparent from the data presented here. During MS analysis the SCs fragmented under conditions that do not induce fragmentation in fragile gold-thiolate SCs.[49] The IBANs were also somewhat prone to aggregation during SV-AUC analysis, another gentle technique that does not adversely affect gold-thiolate SCs.[54] Gold-thiolate protecting groups have been demonstrated to be sensitive to electron transfer, leading to structural rearrangement and increased ligand exchange rates.[9,74-76] The evidence presented here indicates that the silver-thiolate interface is even more sensitive to its electronic environment, thus favouringa uniquelythiolate-rich structure.

Conclusion

Previously-described arylthiolate-protected silver IBANs have been discovered to be a highly monodisperse silver-thiolate superatom complex with a molecular formula of $Ag_{44}(SR)_{30}^{4-}$. Thus the remarkable optical properties of IBANs can be connected to a single species. The identification of a molecular identity for the IBANs is expected to lead to greater confidence in structural predictions, and increased understanding of the relationship between silver-thiolate and gold-thiolate SCs. A better understanding of the source of lability in IBANs should also lead to improved synthetic methods, allowing further study and application development.

Supplementary Material

Refer to Web version on PubMed Central for supplementary material.

Acknowledgments

Financial support for this work was provided by the National Institutes of Health (RC2DA028981), the National Science Foundation (NSF 0903787), the Defense Threat Reduction Agency (HDTRA1-09-0013), the Vanderbilt College of Arts and Sciences, the Vanderbilt Institute of Chemical Biology, the Vanderbilt Institute for Integrative Biosystems Research and Education, and the King Abdullah University of Science and Technology (KAUST) FIC Award (FIC/2010/02).

References

1. Alvarez MM, Khoury JT, Schaaff TG, Shafigullin MN, Vezmar I, Whetten RL. J. Phys. Chem. B. 1997; 101:3706–3712.
2. Negishi Y, Takasugi Y, Sato S, Yao H, Kimura K, Tsukuda T. J. Am. Chem. Soc. 2004; 126:6518–6519. [PubMed: 15161256]
3. Aikens CM. J. Phys. Chem. C. 2008; 112:19797–19800.
4. Jin R. Nanoscale. 2010; 2:343–362. [PubMed: 20644816]
5. Chen SW, Ingram RS, Hostetler MJ, Pietron JJ, Murray RW, Schaaff TG, Khoury JT, Alvarez MM, Whetten RL. Science. 1998; 280:2098–2101. [PubMed: 9641911]
6. Aikens CM. J. Phys. Chem. Lett. 2010; 2:99–104.
7. Jadzinsky PD, Calero G, Ackerson CJ, Bushnell DA, Kornberg RD. Science. 2007; 318:430–433. [PubMed: 17947577]
8. Heaven MW, Dass A, White PS, Holt KM, Murray RW. J. Am. Chem. Soc. 2008; 130:3754–3755. [PubMed: 18321116]
9. Zhu MZ, Eckenhoff WT, Pintauer T, Jin RC. J. Phys. Chem. C. 2008; 112:14221–14224.
10. Lopez-Acevedo O, Akola J, Whetten RL, Gronbeck H, Hakkinen H. J. Phys. Chem. C. 2009; 113:5035–5038.

11. Wu Z, Lanni E, Chen W, Bier ME, Ly D, Jin R. J. Am. Chem. Soc. 2009; 131:16672–16674. [PubMed: 19886625]
12. Xiang H, Wei S-H, Gong X. J. Am. Chem. Soc. 2010; 132:7355–7360. [PubMed: 20462214]
13. Dass A. J. Am. Chem. Soc. 2011; 133:19259–19261. [PubMed: 22077797]
14. Qian H, Zhu Y, Jin R. Proc. Natl. Acad. Sci. 2012; 109:696–700. [PubMed: 22215587]
15. Negishi Y, Chaki NK, Shichibu Y, Whetten RL, Tsukuda T. J. Am. Chem. Soc. 2007; 129:11322–11323. [PubMed: 17715923]
16. Maity P, Xie S, Yamauchi M, Tsukuda T. Nanoscale. 2012 Accepted Manuscript.
17. Alvarez MM, Khoury JT, Schaaff TG, Shafigullin M, Vezmar I, Whetten RL. Chem. Phys. Lett. 1997; 266:91–98.
18. Tracy JB, Crowe MC, Parker JF, Hampe O, Fields-Zinna CA, Dass A, Murray RW. J. Am. Chem. Soc. 2007; 129:16209–16215. [PubMed: 18034488]
19. Tracy JB, Kalyuzhny G, Crowe MC, Balasubramanian R, Choi JP, Murray RW. J. Am. Chem. Soc. 2007; 129:6706–6707. [PubMed: 17477534]
20. Dass A, Stevenson A, Dubay GR, Tracy JB, Murray RW. J. Am. Chem. Soc. 2008; 130:5940–5946. [PubMed: 18393500]
21. Parker JF, Fields-Zinna CA, Murray RW. Acc. Chem. Res. 2010; 43:1289–1296. [PubMed: 20597498]
22. Akola J, Walter M, Whetten RL, Hakkinen H, Gronbeck H. J. Am. Chem. Soc. 2008; 130:3756–3757. [PubMed: 18321117]
23. Schaaff TG, Knight G, Shafigullin MN, Borkman RF, Whetten RL. J. Phys. Chem. B. 1998; 102:10643–10646.
24. Negishi Y, Nobusada K, Tsukuda T. J. Am. Chem. Soc. 2005; 127:5261–5270. [PubMed: 15810862]
25. Hamouda R, Bellina B, Bertorelle F, Compagnon I, Antoine R, Broyer M, Rayane D, Dugourd P. J. Phys. Chem. Lett. 2010; 1:3189–3194.
26. Wu Z, Gayathri C, Gil RR, Jin R. J. Am. Chem. Soc. 2009; 131:6535–6542. [PubMed: 19379012]
27. Branham MR, Douglas AD, Mills AJ, Tracy JB, White PS, Murray RW. Langmuir. 2006; 22:11376–11383. [PubMed: 17154628]
28. Farrag M, Thämer M, Tschurl M, Bürgi T, Heiz U. J. Phys. Chem. C. 2012; 116:8034–8043.
29. Kumar S, Bolan MD, Bigioni TP. J. Am. Chem. Soc. 2010; 132:13141–13143. [PubMed: 20822140]
30. Rao TUB, Nataraju B, Pradeep T. J. Am. Chem. Soc. 2010; 132:16304–16307. [PubMed: 21033703]
31. Negishi Y, Arai R, Niihori Y, Tsukuda T. Chem. Commun. 2011; 47
32. Guo J, Kumar S, Bolan MD, Desireddy A, Bigioni TP, Griffith WP. Anal. Chem. 2012 Just Accepted Manuscript.
33. Walter M, Akola J, Lopez-Acevedo O, Jadzinsky PD, Calero G, Ackerson CJ, Whetten RL, Gronbeck H, Hakkinen H. Proc. Natl. Acad. Sci. U. S. A. 2008; 105:9157–9162. [PubMed: 18599443]
34. Hakkinen H. Chem. Soc. Rev. 2008; 37:1847–1859. [PubMed: 18762834]
35. Reilly SM, Krick T, Dass A. J. Phys. Chem. C. 2010; 114:741–745.
36. Bakr OM, Amendola V, Aikens CM, Wenseleers W, Li R, Dal Negro L, Schatz GC, Stellacci F. Angew. Chem. 2009; 121:6035–6040.
37. Demeler, B.; Gorbet, G.; Zollars, D.; Brookes, E.; Cao, W.; Dubbs, B. UltraScan-III, a comprehensive analysis software for analytical ultracentrifugation experiments. http://www.ultrascan.uthscsa.edu
38. Brookes E, Cao W, Demeler B. Eur. Biophys. J. 2010; 39:405–414. [PubMed: 19247646]
39. Demeler B. Curr. Protoc. Prot. Sci. 2010:7.13.11–17.13.24.
40. Brookes, E.; Demeler, B. Wandrey, C.; Cölfen, H., editors. Vol. 131. Springer Berlin; Heidelberg: 2006. p. 33-40.

41. Brookes, EH.; Demeler, B. presented in part at the Proceedings o f the 9th Annual Conference on Genetic and Evolutionary Computation; London, England. 2007;
42. Demeler B, Brookes E. Colloid Polym. Sci. 2008; 286:129–137.
43. Chaki NK, Negishi Y, Tsunoyama H, Shichibu Y, Tsukuda T. J. Am. Chem. Soc. 2008; 130:8608–8610. [PubMed: 18547044]
44. Dass A. J. Am. Chem. Soc. 2009; 131:11666–11667. [PubMed: 19642643]
45. Knoppe S, Dharmaratne AC, Schreiner E, Dass A, Bürgi T. J. Am. Chem. Soc. 2010; 132:16783–16789. [PubMed: 21067168]
46. Nimmala PR, Dass A. J. Am. Chem. Soc. 2011; 133:9175–9177. [PubMed: 21627117]
47. Qian H, Jin R. Chem. Commun. 2011; 47:11462–11464.
48. Zhu M, Qian H, Jin R. J. Phys. Chem. Lett. 2010; 1:1003–1007.
49. Harkness KM, Cliffel DE, McLean JA. Analyst. 2010; 135:868–874. [PubMed: 20419232]
50. Fields-Zinna CA, Crowe MC, Dass A, Weaver JEF, Murray RW. Langmuir. 2009; 25:7704–7710. [PubMed: 19518136]
51. Kumara C, Dass A. Nanoscale. 2012 Advance Article.
52. Cathcart N, Mistry P, Makra C, Pietrobon B, Coombs N, Jelokhani-Niaraki M, Kitaev V. Langmuir. 2009; 25:5840–5846. [PubMed: 19358597]
53. Angel LA, Majors LT, Dharmaratne AC, Dass A. ACS Nano. 2010; 4:4691–4700. [PubMed: 20731448]
54. Carney RP, Kim JY, Qian H, Jin R, Mehenni H, Stellacci F, Bakr OM. Nat. Commun. 2011; 2:335. [PubMed: 21654635]
55. Shi X-Z, Shen C-M, Wang D-K, Li C, Tian Y, Xu Z-C, Wang C-M, Gao H-J. Chinese Physics B. 2011; 20:076103.
56. Demeler B, van Holde KE. Anal. Biochem. 2004; 335:279–288. [PubMed: 15556567]
57. Demeler B, Saber H, Hansen JC. Biophys. J. 1997; 72:397–407. [PubMed: 8994626]
58. Reimers JR, Wang Y, Cankurtaran BO, Ford MJ. J. Am. Chem. Soc. 2010; 132:8378–8384. [PubMed: 20518461]
59. Dass A. Nanoscale. 2012; 4:2260–2263. [PubMed: 22362222]
60. Qian H, Eckenhoff WT, Zhu Y, Pintauer T, Jin R. J. Am. Chem. Soc. 2010; 132:8280–8281. [PubMed: 20515047]
61. Wang ZW, Toikkanen O, Quinn BM, Palmer RE. Small. 2011; 7:1542–1545. [PubMed: 21495183]
62. Woodruff DP. Phys. Chem. Chem. Phys. 2008; 10:7211–7221. [PubMed: 19060964]
63. Fields-Zinna CA, Sampson JS, Crowe MC, Tracy JB, Parker JF, deNey AM, Muddiman DC, Murray RW. J. Am. Chem. Soc. 2009; 131:13844–13851. [PubMed: 19736992]
64. Allred AL. J. Inorg. Nucl. Chem. 1961; 17:215–221.
65. Price RC, Whetten RL. J. Am. Chem. Soc. 2005; 127:13750–13751. [PubMed: 16201770]
66. Chen S, Murray RW, Feldberg SW. J. Phys. Chem. B. 1998; 102:9898–9907.
67. Fields-Zinna CA, Sardar R, Beasley CA, Murray RW. J. Am. Chem. Soc. 2009; 131:16266–16271. [PubMed: 19845358]
68. Pietron JJ, Hicks JF, Murray RW. J. Am. Chem. Soc. 1999; 121:5565–5570.
69. Ma JC, Dougherty DA. Chem. Rev. 1997; 97:1303–1324. [PubMed: 11851453]
70. Guo R, Georganopoulou D, Feldberg SW, Donkers R, Murray RW. Anal. Chem. 2005; 77:2662–2669. [PubMed: 15828808]
71. Lindeman SV, Rathore R, Kochi JK. Inorg. Chem. 2000; 39:5707–5716. [PubMed: 11151371]
72. Bosch E, Barnes CL. Inorg. Chem. 2002; 41:2543–2547. [PubMed: 11978124]
73. Laibinis PE, Whitesides GM, Allara DL, Tao YT, Parikh AN, Nuzzo RG. J. Am. Chem. Soc. 1991; 113:7152–7167.
74. Song Y, Harper AS, Murray RW. Langmuir. 2005; 21:5492–5500. [PubMed: 15924480]
75. Harkness KM, Fenn LS, Cliffel DE, McLean JA. Anal. Chem. 2010; 82:3061–3066. [PubMed: 20229984]
76. Dass A, Holt K, Parker JF, Feldberg SW, Murray RW. J. Phys. Chem. C. 2008; 112:20276–20283.

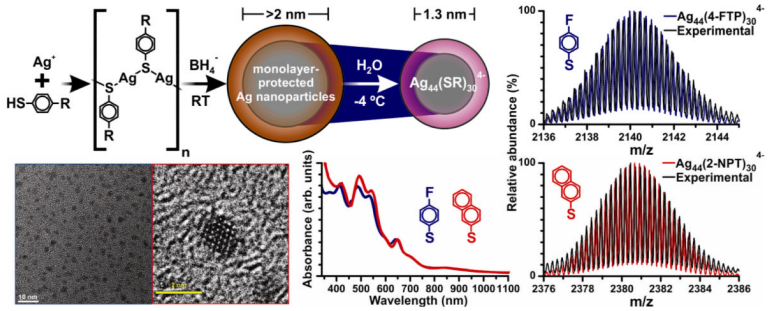

Figure 1.

Synthetic scheme and characterization data for two silver-thiolate superatom complexes, $Ag_{44}(SC_6H_4F)_{30}^{4-}$ (4-FTP IBANs) and $Ag_{44}(SC_{10}H_7)_{30}^{4-}$ (2-NPT IBANs). Characterization data are consistent with previously-reported IBANs,[36] and mass spectra match well with calculated spectra (blue and red, respectively) for the two IBANs.

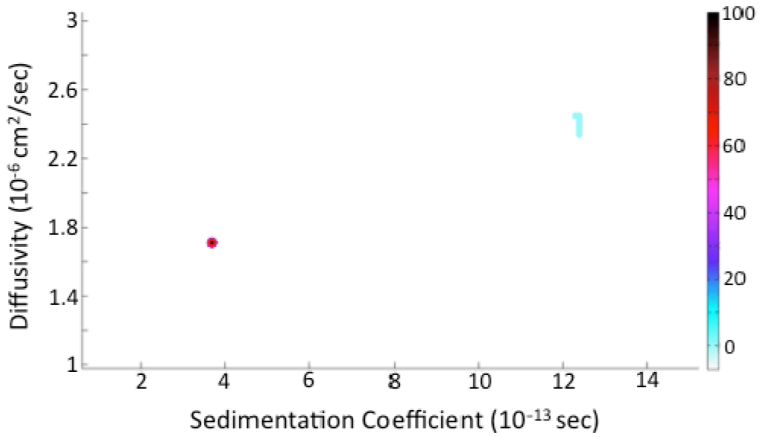

Figure2.

2D plot of sedimentation (*S*) and diffusion (*D*) coefficients of the species present in the 2-NPT IBAN sample. Approximately 94% of the sample concentration is at $s = 3.68\times10^{-13}$ s and $D = 1.7\times10^{-6}$ cm^{2}s^{-1}.

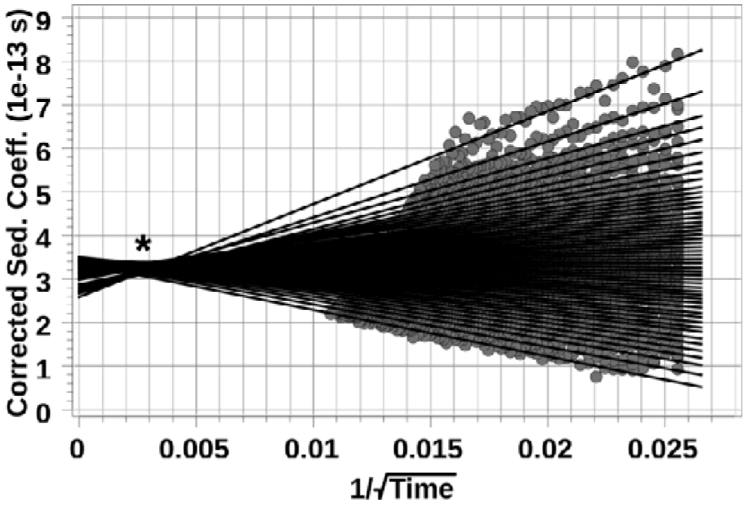

Figure 3.
Extrapolation plot for the enhanced vHW analysis of 2-NPT IBANs. The crossing over of the extrapolation lines at "*" is indicative of slight non-ideal behavior.